Heliyon 10 (2024) e39548

Contents lists available at ScienceDirect

Heliyon

journal homepage: www.cell.com/heliyon

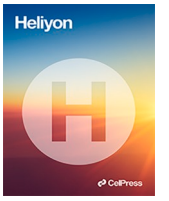

Research article

Sodium arsenite-induced DNA methylation alterations exacerbated by p53 knockout in MCF7 cells

Felicia Fei-Lei Chung [a,b], Rita Khoueiry [a], Aurélie Sallé [a], Cyrille Cuenin [a], Maria Bošković [a,c], Zdenko Herceg [a,*]

[a] Epigenomics and Mechanisms Branch, International Agency for Research on Cancer (IARC), 25 Av. Tony Garnier, 69007, Lyon, France
[b] Department of Medical Sciences, School of Medical and Life Sciences, Sunway University, Jalan University, Bandar Sunway, Subang Jaya, 47500, Malaysia
[c] Institute of Biochemistry II, Faculty of Medicine, Goethe University Frankfurt, Theodor-Stern-Kai 7, 60590, Frankfurt Am Main, Germany

ARTICLE INFO

Keywords:
Environmental carcinogens
Epigenetics
epigenetic stability

ABSTRACT

Epigenetic alterations are ubiquitous across human malignancies. Thus, functional characterization of epigenetic events deregulated by environmental pollutants should enhance our understanding of the mechanisms of carcinogenesis and inform preventive strategies. Recent reports showing the presence of known cancer-driving mutations in normal tissues have sparked debate on the importance of non-mutational stressors potentially acting as cancer promoters. Here, we aimed to test the hypothesis that the presence of mutations in p53, a commonly mutated gene in human malignancies, may influence cellular response to an environmental non-mutagenic agent, potentially involving epigenetic mechanism. We used the CRISPR-Cas9 system to generate knockouts of p53 in MCF7 and T47D breast cancer cell lines and characterized DNA methylome changes by targeted pyrosequencing and methylome-wide Infinium MethylationEPIC BeadChip arrays after exposure to sodium arsenite, a well-established human carcinogen with documented effects on the epigenome. We found that the knockout of p53 alone was associated with extensive alterations in DNA methylation content, with predominant CpG hypermethylation concurrent with global demethylation, as determined by LINE-1 repetitive element pyrosequencing. While exposure to sodium arsenite induced little to no effects in parental cell lines, mutant cells, upon treatment with sodium arsenite, exhibited a markedly altered response in comparison to their wild-type counterparts. We further performed genome regional analyses and found that differentially methylated regions (DMRs) associated with exposure to sodium arsenite map to genes involved in chromatin remodeling and cancer development. Reconstitution of wild-type p53 only partially restored p53-mutant-specific differential methylation states in response to sodium arsenite exposure, which may be due to the insufficient reconstitution of p53 function, or suggestive of a potential exposure-specific epigenetic memory. Together, our results revealed widespread epigenetic alterations associated with p53 mutation that influence cellular response to sodium arsenite exposure, which may constate an important epigenetic mechanism by which tumour promoting agents synergize with driver mutations in cancer promotion.

* Corresponding author.
E-mail address: hercegz@iarc.who.int (Z. Herceg).

https://doi.org/10.1016/j.heliyon.2024.e39548
Received 17 July 2024; Received in revised form 24 September 2024; Accepted 16 October 2024
Available online 18 October 2024

1. Introduction

The accumulation of epigenetic alterations, much like that of genetic alterations, plays a crucial role in the development of human cancers [1,2]. The dysregulation in gene expression resulting from epigenetic reprogramming contribute to the distinctive hallmark capabilities associated with tumour development and malignant progression [3]. A broader appreciation of epigenetic deregulation in the aetiology of human cancer has led to an increasing call for incorporation of epigenetics and epigenomics into carcinogen identification and safety assessment [4,5]. As a wide range of known and suspected human carcinogens (environmental pollutants, physical, and biological agents) have been linked to epigenome deregulation in normal and malignant cells, the ability to induce non-mutagenic epigenetic alterations has been included as one of the key characteristics of carcinogens [6]. Consistent with the notion that the epigenome serves as the interface between the genome and the environment, epigenetic modifications were found responsive to environmental stressors, and are proposed as plausible mechanisms by which environmental factors contribute to carcinogenesis [7, 8].

A comprehensive study of the cancer epigenome has revealed that consistent locus-specific DNA methylation changes differentiate tumour and normal tissue across tumour types, underscoring the universality of epigenetic aberrations in carcinogenesis and malignant progression [9]. Moreover, multiple studies aimed at identifying the factors underlying tumour-specific epigenetic aberrations have demonstrated that deregulation in epigenetic regulatory genes (e.g. *TET1*, *KDM1A,* and *ARID1A*) is consistently enriched in pan-cancer studies [9–11]. Intriguingly, mutations that alter the function or expression of cancer driver genes which encode for proteins not known to directly influence the epigenome (e.g. *IDH1*, *TP53*, *GATA3*, and *PIK3CA*) have also been shown to result in downstream epigenetic deregulation [9,12,13], providing further evidence that the interplay between epigenetic and genetic factors plays a key role in cancer development.

While the advent of large-scale molecular profiling efforts and the integration of exposomic approaches have deepened our understanding of gene-environment interactions and their influence on cancer risk [14,15], more studies are warranted to better outline the impact carcinogenic exposures could have on the epigenome and cellular behaviour, particularly in individuals harbouring genetic alterations that predispose them to cancer. For instance, the discovery that exposure to pervasive environmental toxins such as formaldehyde and acetaldehyde selectively depletes the BRCA2 tumour suppressor protein highlighted the importance of understanding gene-environment interactions [16]. However, to date, it remains to be investigated if a backdrop of genetic alterations will correspondingly alter the epigenome, sensitizing cells exposed to environmental toxins.

Substantial epidemiologic evidence has linked exposure to inorganic arsenic to various human cancers, including lung, skin, and urinary bladder cancers [17–19]. Arsenic is a pervasive environmental toxin, with over 100 million people worldwide estimated to be exposed to carcinogenic levels of arsenic, particularly through the consumption of contaminated drinking water [17]. Arsenite, the common form of arsenic found in water [17,20], is biotransformed in hepatocytes through a series of sequential oxidative-methylation and reduction steps resulting in the production of methylation products including monomethylarsenate, monomethylarsenite, dimethylarsenate, and dimethylarsenite [21]. Excessive arsenic metabolism will lead to the depletion of *S*-adenosylmethionine, which is the principal source of methyl groups to be transferred onto the C5' position of cytosines at CpG dinucleotides by DNA methyltransferases (DNMTs) to produce 5-methylcytosines [21]. Additionally, arsenic has been shown to inhibit DNMTs either by reducing enzyme activity [22–24] or decreasing expression of the enzyme [25], ultimately leading to genome-wide DNA hypomethylation as well as perturbations in histone modification and miRNA levels (as reviewed in [26]). Additionally, exposure to arsenic in early life has been shown to induce global DNA hypomethylation in the children of exposed individuals [27], while genomic regions associated with the tumour suppressor p16 [28], extracellular matrix remodeling genes such as metalloproteinase-9 (MMP-9) and tissue inhibitor of matrix metalloproteinase-1 (TIMP-1) were hypermethylated with increasing exposure to arsenic *in utero* and early life [29]. However, the combined interactions between genetic alterations and environmental exposures on the epigenome have not been well established.

In this study, we reasoned that mutations in cancer drivers not only assume a primary role at different stages of tumorigenesis (and dictate cancer outcome/phenotype) but that they may also enhance the carcinogenic potential of environmental exposures through mutational and non-mutational mechanisms. Specifically, we hypothesized that mutations in common cancer-related genes influence cellular response to environmental exposures. Cells that have a background of genetic aberrations may be more susceptible to epigenetic reprogramming by environmental toxicants.

2. Materials and methods

2.1. Cell culture and CRISPR-Cas9 gene editing

Human breast carcinoma cell lines MCF7 (ATCC) and T47D (ATCC) were maintained in RPMI (Gibco) containing 10 % fetal bovine serum (Gibco), 100 IU/mL penicillin (Gibco), and 100 μg/mL streptomycin (Gibco). All cells were maintained in a 37 °C environment containing 5 % CO_2. Guide RNA targeting p53 were designed using the ThermoFisher GeneArt CRISPR design tool (sequences in Supplemental Table 1) and ligated into the pLenti-Guide-Puro (#GE100032, Origene) CRISPR vector, and positive clones confirmed by Sanger sequencing (Eurofins Genomics). Pools of guide RNA plasmids were subsequently co-transfected with the hCas9 plasmid (#41815, Addgene) into the target cell lines using Lipofectamine 3000 (Invitrogen) according to the manufacturer's instructions. Following puromycin selection, isogenic cell lines were isolated, cultured, and verified as knockouts by Sanger sequencing and Western blot for p53. Sodium arsenite (S7400, Sigma-Aldrich) was prepared in dimethyl sulfoxide (DMSO), and cells were treated with a final concentration of 3 μM sodium arsenite for 72 h. The DMSO-only served as the negative control.

2.2. Determination of cell viability

Cell viability in response to sodium arsenite was quantified using the CellTiter 96® Aqueous One Solution Cell Proliferation Assay (Promega) according to the manufacturer's instructions. Briefly, cells were seeded in 96 well plates overnight before being exposed to treatment with sodium arsenite for 72 h. The CellTiter 96® Aqueous One Solution Reagent was then added to each well and incubated for a further 4 h. The absorbance of the resulting bioreduced formazan product was measured at 492 nm using an Apollo 11 LB913 plate reader.

2.3. Reconstitution of full-length p53

pcDNA3 expression vector containing cDNA coding for wild-type p53 (pcDNA-p53^{WT}) was received as a kind gift from Dr Magali Olivier. Cells (2 x 10^5) cells were transfected with 5 μg of the pcDNA-p53^{WT} plasmid using the Xfect transfection reagent (Takara Bio) according to the manufacturer's instructions. Positive clones were selected using 1 mg/mL G418.

2.4. Protein extraction and immunoblot analysis

Total cell lysates were prepared using ice-cold RIPA-like buffer supplemented with protease inhibitors (50 mM Tris pH 7.4, 250 mM NaCl, 0.1 % SDS, 2 mM DTT, 0.5 % NP-40NP40 and 1X cOmplete Protease Inhibitor, Roche). Proteins (50 μg/well) were separated on 4–15 % Mini-PROTEAN TGX Precast Protein Gels (Bio-Rad) and transferred onto polyvinylidene fluoride membrane (Bio-Rad) with the Trans-Blot SD Semi-Dry Transfer Cell (Bio-Rad) at 18 V for 60 min. Membranes were blocked with 5 % skimmed milk in 1X Tris-Buffered Saline, 0.1 % Tween-20 (TBST) solution for 2 h at room temperature with gentle agitation and then incubated overnight with the primary antibody at 4 °C with gentle agitation. Anti-p53 (1:2000, sc-126 Santa Cruz Biotechnology) and anti-GAPDH (1:2000, sc-32233 Santa Cruz Biotechnology) primary antibodies were used in this study. Species-matched horseradish peroxidase-conjugated secondary antibodies (1:5000) were used to enable detection using the Clarity Western ECL mix (Bio-Rad).

2.5. Methylome-wide profiling and data analysis

Total DNA and RNA were extracted using the Qiagen AllPrep DNA/RNA Kit.

The quantity and quality of nucleic acids were determined using a Qubit 4 instrument (Thermo Fisher Scientific). Extracted DNA (500 ng) was subjected to bisulfite conversion using the EZ DNA Methylation Kit (Zymo Research). The bisulfite-modified DNA was analyzed using the Infinium MethylationEPIC BeadChip arrays, which assess DNA methylation levels at more than 850,000 CpG sites (Illumina). The data was analyzed using the methylkey pipeline developed by the Epigenomics and Mechanisms Branch at the International Agency for Research on Cancer (https://github.com/IARCbioinfo/methylkey). Briefly, raw data files were pre-processed, in which background correction was conducted by normal-exponential out-of-band (Noob), normalization of signal intensity values by the SWAN normalization method, and quality control was performed using the *minfi* R package [30]. As the samples were processed in a way that no significant batch effects affecting the intergroup comparisons were observed, batch correction was not applied to this dataset. Intergroup comparisons were conducted using robust linear regression analysis as implemented in the *limma* R package. Differentially methylated probes (DMPs) were defined as those that were significantly different between the compared groups with a false discovery rate-adjusted p-value of <0.05 and with an intergroup absolute mean beta value difference of >10 %. Regional analysis to identify differentially methylated regions (DMRs) was conducted using the *DMRcate* R package. Plots reflecting the quality of the signal intensities are shown in Supplemental Figs. 1A and 1B. The potential impact of sentrix ID, which may contribute towards batch effects, was evaluated by multidimensional scaling shown in Supplemental Fig. 1C. Pathway enrichment analyses were conducted using the Enrichr tool [31–33]. Plots were generated using the *ggplot2* [34] and *ggridges* [35] R packages. The *REMP* R package was used to estimate DNA methylation levels at CpG sites mapped to LINE-1 repetitive elements [36].

2.6. LINE-1 pyrosequencing

LINE-1 pyrosequencing was used for the quantitative measurement of DNA methylation levels in 5 CpG sites associated with LINE-1 sequences, as previously described [37,38]. Briefly, 500 ng of DNA was subjected to sodium bisulfite modification using the EZ DNA Methylation-Gold Kit (Zymo Research) according to the manufacturer's instructions. Amplification of LINE-1 regions was performed using the HotStarTaq Master Mix kit (Qiagen), and pyrosequencing was carried out using the PyroMark Q96 ID pyrosequencing system (Qiagen) following the manufacturer's protocol. Methylation states at the target CpGs were evaluated by calculating the average of all CpG sites analyzed at the LINE-1 region.

2.7. RT-qPCR analysis

RT-qPCR gene expression analysis of p53 target genes was performed as previously described, with modifications [39]. Briefly, total RNA was converted to cDNA using MMLV-RT and oligo(dT) primers (Invitrogen). Gene expression levels were quantified by CFX96 PCR detector system (Bio-Rad) using the SsoAdvanced Universal SYBR Green Supermix (Bio-Rad). The PCR conditions used were as follows: 94 °C for 3 min, followed by 40 cycles of 94 °C for 40 s, 60 °C for 40 s and 72 °C for 25 s. Primers used are as indicated in Supplemental Table 2. Glyceraldehyde-3-phosphate dehydrogenase (GAPDH) was used as the housekeeping gene for normalization.

3. Results

3.1. Loss of TP53 results in global demethylation in MCF7 cell lines and alters cellular response to sodium arsenite treatment

To test the hypothesis that mutations in common cancer driver genes may influence cellular response to environmental exposures, we investigated the impact of p53 mutation on cellular response to sodium arsenite, a derivative of arsenic, which in turn is a well-established human carcinogen with reported epigenetic modifying properties [40]. To this end, we generated MCF7 breast cancer cell lines harbouring mutant p53 using CRISPR-Cas9 gene editing and analyzed the methylome for sodium arsenite-exposed p53 knockout (KO) cells and their wild-type counterparts (Fig. 1A). The two independent MCF7 p53 KO sublines harbored mutations in the p53 coding sequence that resulted in the encoding of premature stop codons (Fig. 1B, Supplemental Fig. 1D), and displayed reduced expression of known p53 target genes GADD45A and CDKN1A (Supplemental Fig. 1E), consistent with the disruption of the p53 gene. To characterize potential DNA methylome changes associated with p53 loss, we profiled the DNA methylome of MCF7 p53 knockout and wild-type cells using the Illumina Infinium MethylationEPIC BeadChip. Substantial differential methylation was observed in the

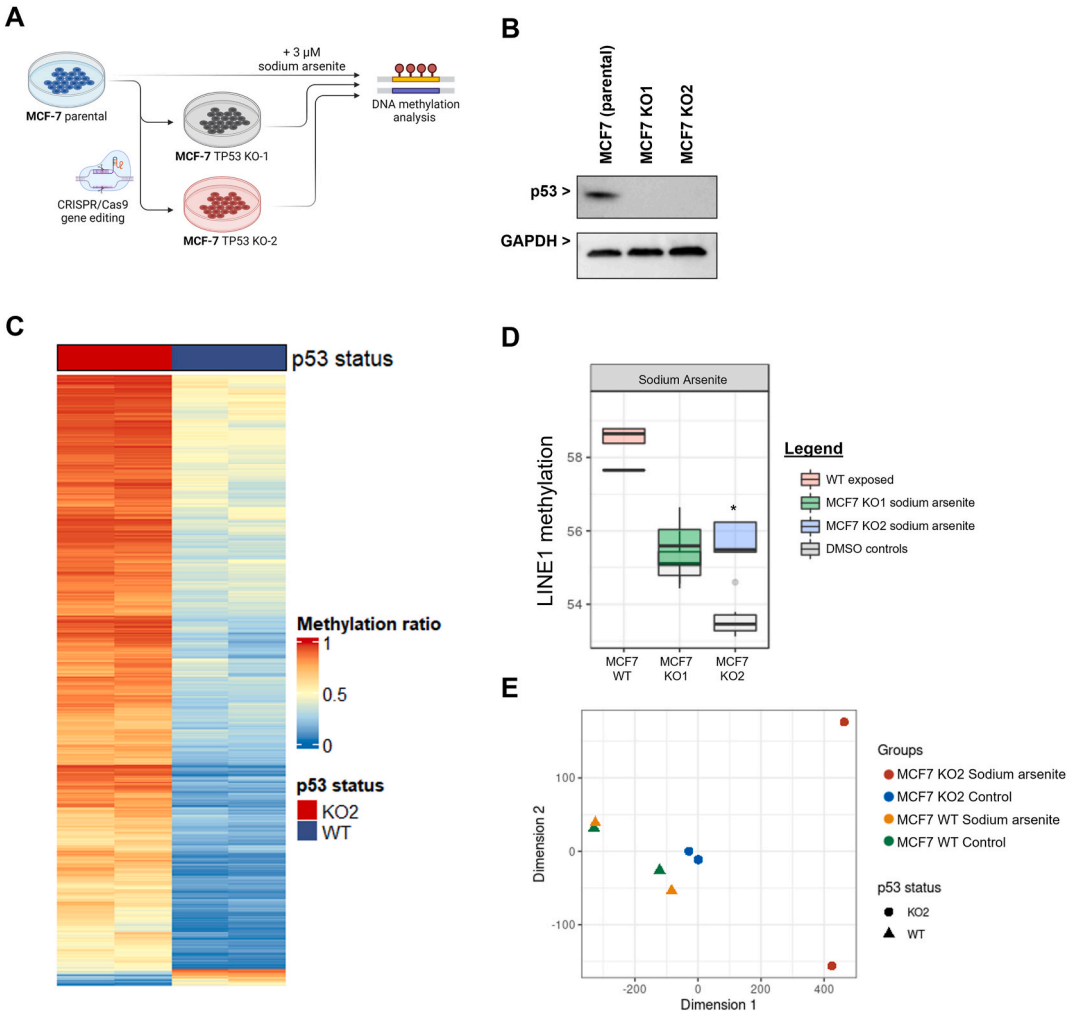

Fig. 1. Loss of p53 expression results in extensive DNA methylation changes and increased sensitivity to sodium arsenite-induced DNA methylation changes. (A) Epigenetic stability was assessed by generating p53-knockout breast cancer cell lines and comparing the effects of sodium arsenite on the epigenome between edited and parental cell lines. Figure created with BioRender.com **(B)** Western blot analysis was conducted to confirm the knockout (KO) status of MCF7 cell lines. **(C)** Heatmap illustrating CpG sites that were consistently differentially methylated in between p53-knockout and wildtype cell lines. **(D)** Analyses of LINE-1 repetitive regions indicate a reduction in DNA methylation in p53-knockout cells relative to the parental cells. Results shown are the mean of five readings per condition. Treatment with 3 µM sodium arsenite resulted in hypermethylation of LINE-1 repetitive regions, which were more pronounced in knockout cells compared to parental MCF7. There was a statistically significant difference between sodium arsenite-treated KO2 cells relative to untreated controls (Student's *t*-test, $p < 0.05$). **(E)** MDS plot illustrating the separation of parental (WT) MCF7 cells and knockout (KO2) cells that were analyzed at an epigenome-wide level with treatment of 3 µM sodium arsenite and untreated controls.

knockout lines relative to the wild-type cells, with significant differential methylation observed in 107,920 CpG sites, of which 99,165 were hypermethylated and 8755 were hypomethylated (Supplemental Table 3, Fig. 1C). Regional analyses comparing p53-KO to wild-type cells yielded 19,505 DMRs, with the topmost differentially methylated genes including p53 target NOTCH4, tumour suppressor T-box 5 (TBX5), and pioneer factor Forkhead box protein A1 (FOXA1) (Supplemental Table 4). Pathway enrichment analyses conducted on differentially methylated regions (DMRs) revealed that the SLC family-related genes, which have also been implicated in cancers, were significantly deregulated upon p53 depletion (Supplemental Table 5). While transcriptome-wide analyses were not conducted in this study, significant downregulation was observed in the genes *integrin subunit beta like 1* (ITGBL1) and *peptidyl arginine deiminase 4* (PADI4), both of which were primarily hypermethylated in MCF7 p53 KO2 (Supplemental Fig. 1F).

In a separate analysis, assessments of global methylation using LINE-1 pyrosequencing revealed a global DNA methylation loss in p53 knockout cells (Fig. 1D, grey whisker-box plots). To examine the impact of exposure to environmental carcinogens on the methylome of cells lacking p53, we exposed p53 KO cells and their wild-type counterparts to sodium arsenite. While knockout and wild-type cells did not display significant differences in cell viability when treated with sodium arsenite (Supplemental Fig. 1G), the treatment at sublethal doses (3 μM) induced hypermethylation of LINE-1 repetitive elements in wild-type and knockout cells (Fig. 1D, coloured whisker-box plots) relative to untreated controls (Fig. 1D, grey whisker-box plots), though this was only statistically significant for the MCF7-KO2 cell line (Student's *t*-test, $p < 0.05$). As the MCF7-KO2 subline was observed to be more dysregulated upon

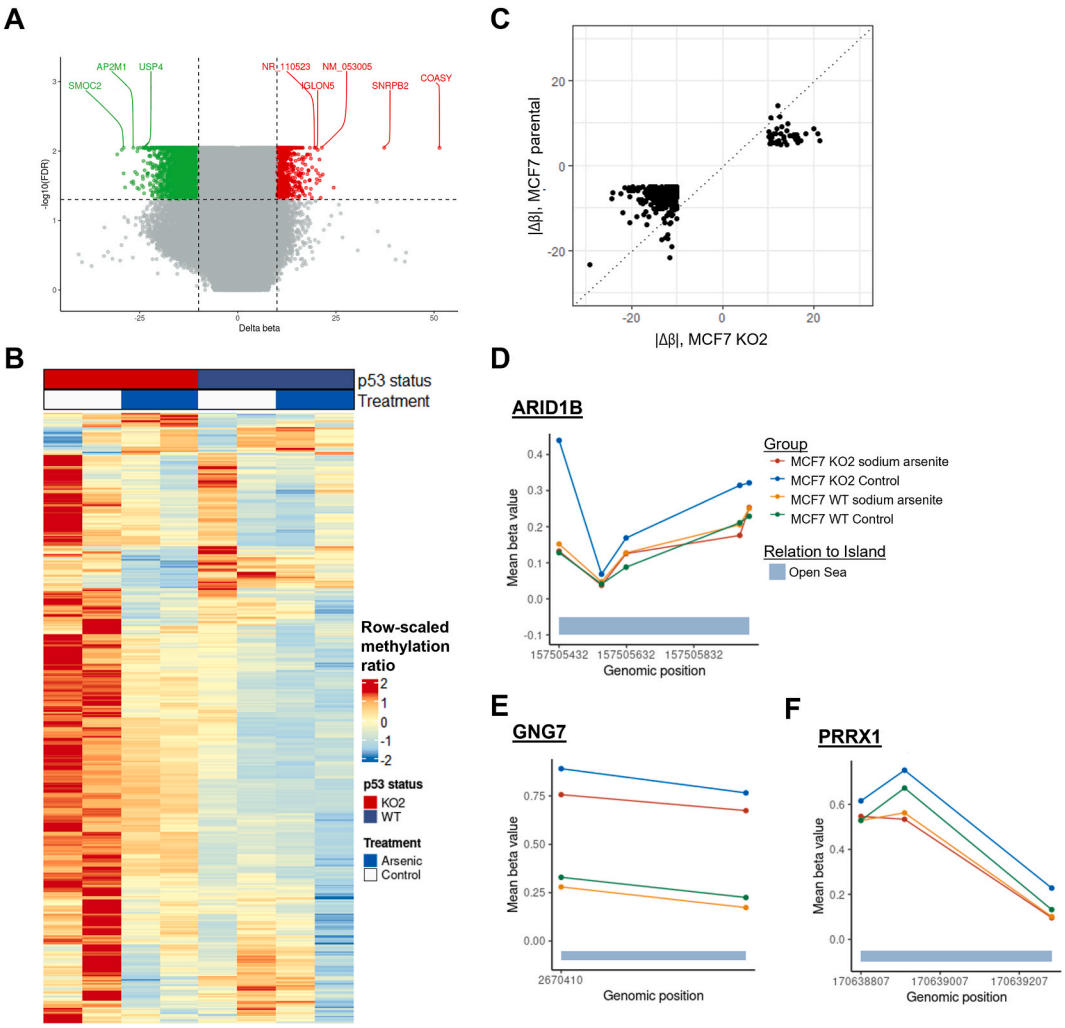

Fig. 2. Sodium arsenite treatment predominantly triggered hypomethylation in treated cells, to which cells depleted for p53 displayed greater sensitivity. (A) Volcano plot illustrating epigenetic changes resulting from 3 μM sodium arsenite treatment in MCF7-KO2. **(B)** Heatmap illustrating differentially methylated probes (DMPs) that were consistently differentially methylated in MCF7-KO2 and parental cell lines, which were predominantly hypermethylated in the knockouts **(C)** Scatterplot comparing the absolute group mean differences ($|\Delta\beta|$) in the probes consistently differentially methylated by sodium arsenite in MCF7 parental and MCF7-KO2 lines indicate that epigenetic alterations were exacerbated in KO lines. Regional plots of DMRs associated with **(D)** ARID1B, **(E)** GNG7, and **(F)** PRRX1 which were identified in sodium arsenite-treated MCF7-KO2 cells.

sodium arsenite treatment, subsequent epigenome-wide analyses were conducted using this subline. Multidimensional scaling of the top 10,000 most variable positions indicated that relatively small variation was observed amongst wild-type control, wild-type sodium arsenite-treated, and KO2 control cells, compared to the KO2 sodium arsenite-treated cells (Fig. 1E).

Probe-level analyses revealed that sodium arsenite treatment resulted in significant differential methylation at 9,098 CpG sites in the MCF7 KO2 subline, of which 8,243 were hypomethylated in treated cells relative to the untreated KO2 controls (Fig. 2A, Supplemental Table 6). Pathway enrichment analyses indicated that genes associated with the top 500 hypermethylated hypomethylated probes included genes involved in the neuronal system (CAMK2B, GRIA2, and GRIK3, Supplemental Table 7). While not statistically significant after adjusting for multiple testing, hypermethylated DMPs were enriched for genes involved in CREB phosphorylation (Supplemental Table 7).

In contrast, no individual CpG sites were significantly differentially methylated based on the same cut-offs in p53-WT MCF7 treated at the same dose of sodium arsenite relative to the untreated p53-WT MCF7 (Supplemental Fig. 1H). Applying less stringent cut-offs (absolute delta betas of >5 % between groups, though the differences do not reach statistical significance), 12,350 probes were observed to be hypomethylated, while 9,804 probes were observed to be hypermethylated in the sodium arsenite-treated group relative to the control (Supplemental Table 8). Overall, these results suggest that the epigenetic effects of sodium arsenite generally result in DNA hypomethylation, the magnitude of which is p53 state-dependent.

3.2. Exposure to sodium arsenite alters DNA methylation states at genes associated with chromatin remodeling and cancer development

In sodium arsenite-treated p53-WT MCF7 cells relative to untreated cells, we identified 14 differentially methylated regions (DMRs), which included hypomethylation in regions associated with adaptive splice regulator *RNA-binding motif protein 20* (RBM20), regulator of transforming growth factor beta receptor binding *Sorting Nexin 25* (SNX25) and PKC-related serine/threonine-protein kinase *Protein kinase N2* (PKN2) (Supplemental Table 9). In p53-KO cells treated in the same manner, 216 DMRs were identified. While not statistically significant following adjustment for multiple testing, pathways enriched in DMRs identified in sodium arsenite-treated p53-KO cells included genes associated with neurotransmission (i.e. PDE10A and PDE5A, Supplemental Table 9), and Nef and signal transduction (i.e. PKN2, Supplemental Table 10) in sodium arsenite-treated wild-type cells, all of which have also been implicated in cancers [41–45].

To identify sodium arsenite-responsive regions that are common to both KO and wild-type cell lines, we intersected probes that were observed to be consistently differentially methylated in p53-KO2 arsenite-treated cells (q-value <0.05 and absolute delta betas >10 %) with wild-type arsenite-treated cells (delta betas >5 % in the same direction as the p53-MCF7 KO2 treated cells). We found 500 probes to be consistently differentially methylated, the majority (454) of which were hypomethylated. Taken together with probe-level comparisons of sodium arsenite-treated cells in the MCF7 KO2 subline presented earlier, which showed the majority of treated DMPs being hypomethylated, these findings showed that sodium arsenite exposure primarily induced hypomethylation regardless of p53 status (Fig. 2B).

The magnitude of differential methylation was greater in the majority of these consistent probes in the MCF7 KO2 cells (485/500), further indicating that arsenite-induced DNA methylation changes are exacerbated in knockout cell lines (Fig. 2C). Fig. 2D–F illustrates the methylation states at DMRs associated with chromatin remodeler and tumour suppressor; *AT-rich interactive domain-containing protein 1B* (ARID1B), tumour suppressor *G protein gamma 7* (GNG7), and transcription factor Paired Related Homeobox 1 (PRRX1), which were identified as significantly different between p53-KO and wild-type parental cells. In these DMRs, sodium arsenite-induced alterations of DNA methylation were greater in magnitude in p53-KO cells than in wild-type parental cells.

3.3. Gene reconstitution of wild-type p53 only partially restores epigenetic stability in MCF7-KO2 cells

Because epigenetic changes are potentially reversible, we reasoned that the changes in DNA methylation resulting from the introduction of mutant p53 may be reversible after reconstitution of functional p53. To determine if the restoration of functional (wild-

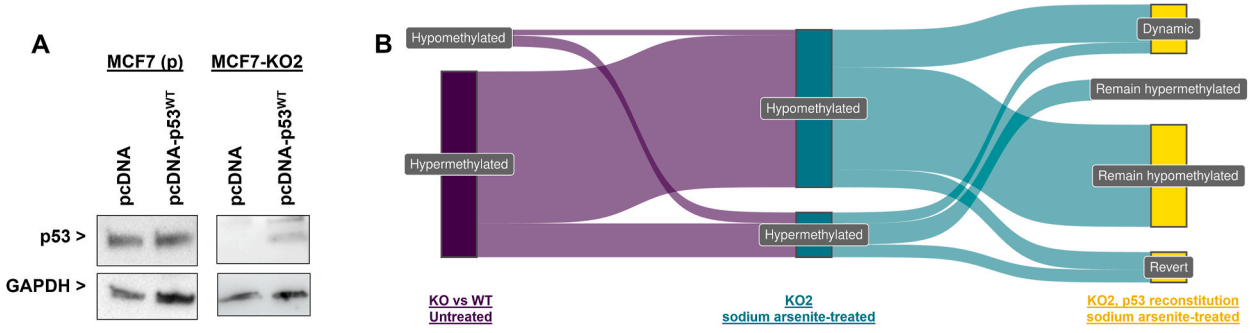

Fig. 3. Reconstitution of p53 is insufficient for restoring epigenetic stability. (A) Wildtype p53 was reconstituted in the MCF7 p53-KO cell lines. **(B)** Sankey plot illustrating the transition between methylation states of differentially methylated probes upon treatment with sodium arsenite and p53 reconstitution. Probes that have 'reverted' refer to probes that were within 5 % by beta value of sodium arsenite-treated parental cells.

type) p53 will reverse the effects of p53 depletion on the methylome, p53-expressing cells (pcDNA-p53^{WT}) were generated in the MCF7-KO2 lines (Fig. 3A). The Sankey plot in Fig. 3B summarizes the transition in methylation states for the probes that were initially found to be differentially methylated in MCF7-KO2 cells relative to the wild-type parental cells (99,165 hypermethylated and 8,755 hypomethylated DMPs). Treatment with sodium arsenite resulted in the hypomethylation of a substantial fraction of the DMPs (81,166 of the 99,165 p53-KO hypermethylated DMPs). Upon reconstitution of p53, probes that had "reverted" to the state observed in p53-WT cells were defined as probes which were within 5 % by beta value of the MCF7 wild-type parental cells treated with sodium arsenite or had been significantly altered towards the methylation state of the arsenite WT-treated cells. The reverted CpGs made up a minority of the analyzed probes, indicating that stable p53-re -expression is insufficient to reverse the effects of depletion of p53, and the subsequent arsenite-induced DNA methylation changes. However, this observation may be due to the fact that p53 was not fully reconstituted to the levels expressed in the parental cell line.

3.4. T47D p53-mutant cell lines exhibit reduced sensitivity to sodium arsenite-induced epigenetic reprogramming

To determine if depletion of mutant p53 will result in similar epigenetic destabilization, knockout clones were generated in T47D cells. These cells were selected because they represent the same molecular subtype of breast cancer as MCF7 (luminal A) while harbouring the p.L194F p53 mutation. Amino acid substitution L194F of p53 is located within the DNA binding domain of the protein conferring a decreased p53 transactivation activity and decreased binding to its partner proteins in cells [46]. Two edited clones were established (Fig. 4A, Supplementary Fig. 2C) and subjected to sodium arsenite treatment similar to the MCF7 cells described previously. Multidimensional scaling of the top 10,000 most variable positions indicated that relatively small variation was observed between sodium arsenite-treated and untreated cells, while relatively large differences were observed between knockout and parental cells (Fig. 4B).

Correspondingly, knockdown clones exhibited substantial differential methylation compared to the parental cell lines (112,793 DMPs in T47D-KO1, and 119,809 DMPs in T47D-KO2; Fig. 4C and E respectively, Supplemental Tables 11 and 12 respectively). Notably, while T47D-KO1 and T47D-KO2 were independent knockout clones, we observed that approximately half of the sodium arsenite-induced hypermethylated sites and the majority of hypomethylated sites were common between these two cell lines (Fig. 4E). Sodium arsenite treatment induced significant differential methylation at 9 CpGs in the parental T47D cells (Supplemental Table 13). Knockout cell lines were slightly sensitized to sodium arsenite treatment and were differentially methylated at 37 and 15 CpGs sites

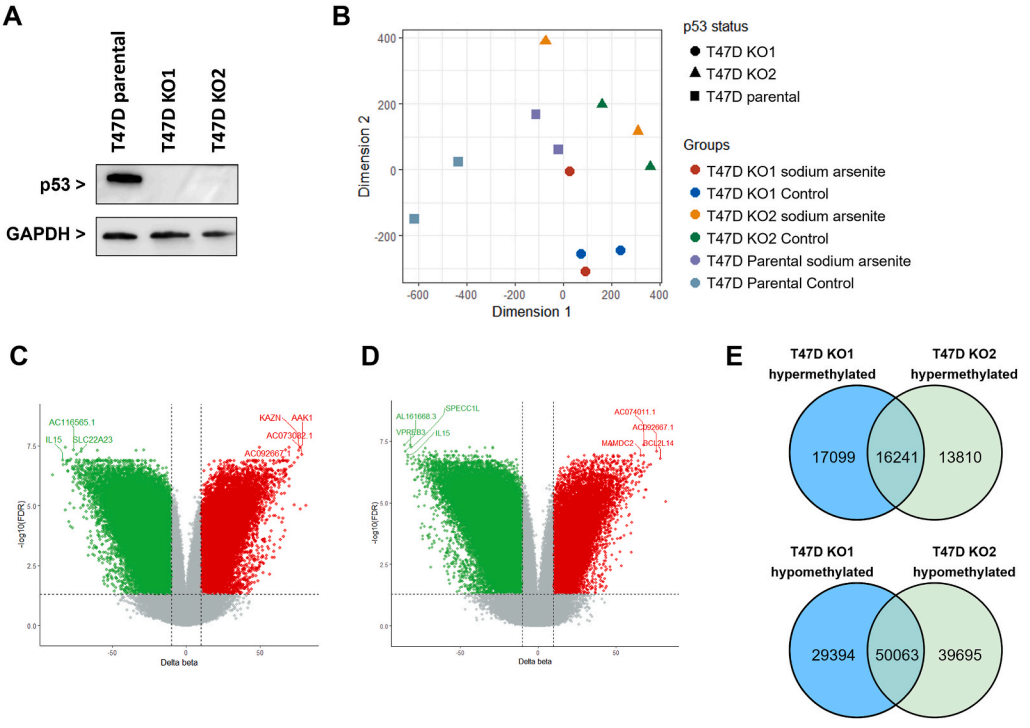

Fig. 4. T47D p53-mutants demonstrate diminished sensitivity to sodium arsenite-induced DNA methylation reprogramming. (A) Western blot analyses was conducted to confirm the knockout status of T47D cell lines. **(B)** MDS plot illustrating the separation of parental (WT) T47D cells and knockout (KO) cells that were analyzed at an epigenome-wide level with treatment of 3 μM sodium arsenite and untreated controls. Volcano plots illustrating DMPs detected when comparing parental T47D to **(C)** T47D KO1 and **(D)** T47D KO2. **(E)** Venn diagrams illustrating the overlap between hyper- and hypomethylated probes detected in T47D KO1 and KO2 lines relative to parental T47D.

respectively (Supplemental Tables 14 and 15).

The overall distribution of beta values in all cell types and treated conditions recapitulated the main findings of the study (Supplementary Fig. 3A), whereby p53 depletion predominantly induced hypermethylation, while arsenic treatment resulted predominantly in hypomethylation in MCF7 cells. T47D parental cells exhibited lower levels of baseline methylation relative to MCF7 parental cells. In contrast to MCF7 cells, depletion of p53 in T47D induced hypomethylation, while treatment with arsenic had minimal effects on the T47D cells regardless of their p53 status. Correspondingly, estimations of DNA methylation at LINE-1 repetitive elements using the *REMP* R package showed that MCF7 p53-KO2 were hypermethylated relative to the parental cells (Supplementary Figs. 3B and 3C), while p53-KO T47D cells exhibited hypomethylation relative to the parental cells (Supplementary Figs. 3B and 3D). These findings contradict the results obtained by LINE-1 pyrosequencing performed on MCF7 cells (described in Fig. 1D), indicating that the LINE-1 pyrosequencing assay may lead to an incomplete assessment of global DNA methylation levels. However, in the absence of comprehensive epigenome-wide profiling methods, the LINE-1 pyrosequencing assay remains a valuable tool for identifying conditions that perturb the epigenome and experimental conditions for more in-depth investigation.

4. Discussion

Major international sequencing efforts have shed light on the comprehensive genomic portraits of common human cancers, revealing a relatively small number of "driver" genes and many passengers (functionally inert mutations). Interestingly, more recent reports showing the presence of known cancer-driving mutations in normal tissues have sparked debate on the importance of tumour promotion that may be enabled by environmental exposures potentially acting through non-mutational mechanisms [47]. The possibility that tumour-promoting agents may synergize with driver mutations by acting through epigenetic mechanisms and fuelling epigenome changes that are rampant in human malignancies has not been investigated. The tumour suppressor gene *TP53* plays a prominent role in modulating cellular response to acute stress, supporting DNA repair by inducing cell cycle arrest or apoptosis in response to DNA damage and controlling a broad range of cellular processes through its activity as a transcription factor [48]. Additionally, it has been demonstrated that mutant forms of p53 proteins may alter cellular mechanisms through gain-of-function interactions [49,50], disrupting genomic stability to a greater degree than in p53 null cells [51]. p53 has also been implicated in the regulation of epigenetic (DNA methylation) machinery [52]. A recent study has reported that mutant p53 protein intersects with epigenetic regulation as mutant p53 tumour cells exhibit differential chromatin accessibility compared to wild-type p53 tumours, suggestive of the role of p53 in mediating these chromatin changes. However, the role of p53 in epigenome regulation during cellular response to stress conditions has yet to be fully elucidated [53].

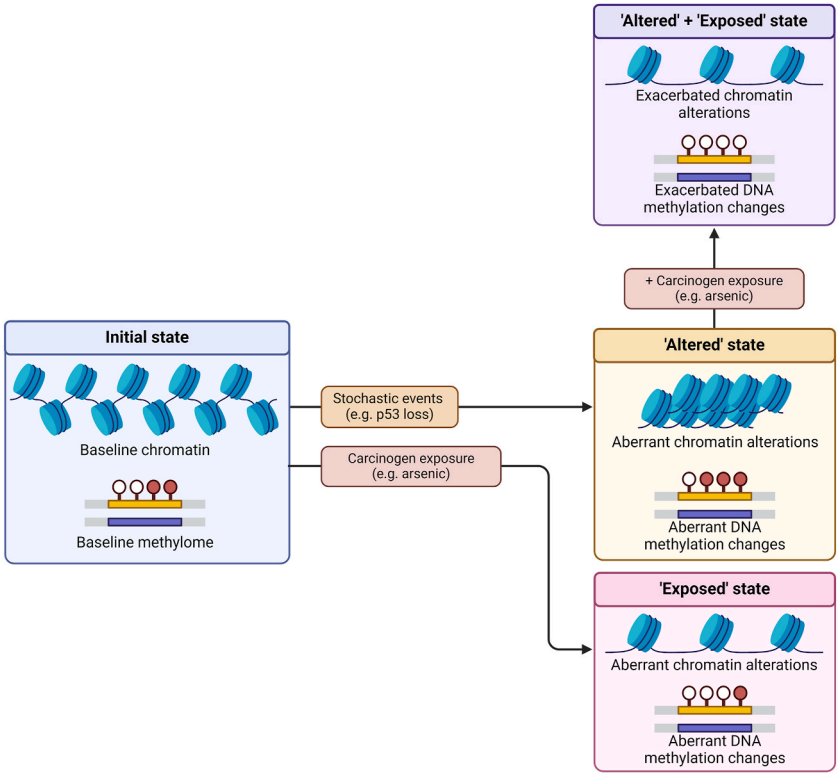

Fig. 5. Proposed mechanistic model of deregulation epigenome stability in response to cancer-promoting exposures in p53 mutant cells. Figure created with BioRender.com.

In this study, we determined that p53 depletion results in extensive alterations to the DNA methylome. Notably, compared to parental cell lines, the epigenome of p53-knockout cells was more severely perturbed following treatment with sodium arsenite, a substance which has been linked to various human cancers, including lung, skin, and urinary bladder cancers [17–19]. By inhibiting DNMTs or by reducing enzyme activity, sodium arsenite treatment is expected to induce genome-wide DNA hypomethylation (as reviewed in [26]). Correspondingly, sodium arsenite predominantly triggered demethylation in treated cells, regardless of p53 status. We observed that although T47D cells and their corresponding knockout lines were less responsive to sodium arsenite treatment, knockout lines derived from both T47D and MCF7 displayed greater sensitivity to sodium arsenite treatment compared to their parental cell lines.

Additionally, we observed that CpG sites that were perturbed due to p53 knockout were sensitive to further alterations induced by sodium arsenite treatment. Partial reconstitution of wild-type p53, however, did not sufficiently rescue the epigenome and did not fully revert differentially methylated sites to that of sodium arsenite-treated parental cells. These observations may have been due to the incomplete reconstitution of wild-type p53 in transfected cells. It may also have been due to lasting effects on the epigenome configuration following p53 depletion.

Epigenome (chromatin) organization has been proposed as a major determinant not only of gene expression programmes but also of the cancer mutational landscape [54,55]. Changes in the epigenomic patterns as a consequence of environmental exposure combined with a driver (p53) or epigenetic driver gene (epidriver) [10] disruption may not only contribute to changes in the transcriptional programme but also enhance the carcinogenic potential of environmental exposures through mutational and non-mutational mechanisms. Indeed, we observed differential methylation in cancer-related genes such as PRRX1 and ARID1B to be more exacerbated in knockout cell lines, which suggests that alterations in cancer driver genes may promote epigenetic deregulation in response to epigenome-modifying exposures (mechanistic model is illustrated in Fig. 5). This may be an alternative mechanism by which chromatin modifiers have been reported to influence mutation density and patterns, through their direct involvement in DNA repair [56]. The mechanisms by which p53 loss impacts epigenome stability may be directly linked to the DNA methylome and may involve p53-mediated regulation of DNA methylation machinery (notably the expression of the *de novo* DNA methyltransferases DNMT3A/DNMT3B and DNA demethylation enzyme TET1/TET2) [57]. Alternatively, although not mutually exclusive to the previously-described mechanism, p53 may impact the methylome profiles indirectly through changes in chromatin accessibility and modification patterns that are known to be linked to the establishment and maintenance of DNA methylation linked to gene activity state.

Interestingly, the findings of DNA methylome instability associated with p53 loss were not fully recapitulated in the T47D cell line model which harbours the p53 p.L194F mutation. Our observations suggest that the p.L194F mutant may play a larger role than initially anticipated in modulating epigenetic states, as evidenced by the widespread alterations following its depletion. However, the mutant cell lines were found to be inherently less responsive to sodium arsenite exposure, with relatively few significant alterations observed between treated and untreated cells regardless of p53 status. With the growing body of evidence highlighting the roles that gain-of-function p53 mutants play in influencing cell behaviour and driving carcinogenesis [50,58,59], it is probable that the presence or absence of each p53 mutant will have a unique impact on the epigenome and the epigenome's response to environmental exposures. Further studies to fully elucidate the differential epigenetic effects of p53 mutants may yield additional information on the effect of different p53 variants on the epigenome and epigenetic stability. Moreover, the relative resistance of T47D cells to sodium arsenite-induced hypomethylation could be attributed to their inherently low baseline levels of DNA methylation. However, it should be noted that T47D exhibited hypomethylation upon p53 knockout, and the observations of Supplementary Fig. 3A indicate that a substantial proportion of CpG sites remain fully or almost fully methylated in all observed conditions. Thus, it is likely that T47D cells possess an intrinsic resistance to sodium arsenite, independent of p53-related mechanism.

A notable limitation of this study was that transcriptome-wide analysis was not performed alongside the methylome-wide analysis. Although differential methylation was observed in genes associated with tumour development, it remains uncertain whether these changes will lead to corresponding shifts in gene expression. However, since this study primarily focused on assessing the impact of mutations on the epigenome and epigenetic stability against perturbations, the impact of the above on the transcriptome was considered beyond its scope. Further studies aimed at gaining insights into the precise mechanisms underlying p53-mediated regulation of the epigenome, including the response to environmental exposure and its impacts on gene expression are warranted.

5. Conclusion

In summary, our study demonstrated that p53 depletion results in persistent alterations to the epigenome that may be only partially rescued by the restoration of wild-type p53 expression. These persistent alterations include the disruption of epigenetic stability and may sensitize cells to epigenetic aberrations induced by environmental exposures. However, further studies will be required to fully understand the implications these findings may have on human health and safety assessments of epigenetic modulators.

CRediT authorship contribution statement

Felicia Fei-Lei Chung: Writing – original draft, Methodology, Investigation, Formal analysis, Data curation, Conceptualization. **Rita Khoueiry:** Writing – original draft, Methodology, Conceptualization. **Aurélie Sallé:** Methodology, Investigation. **Cyrille Cuenin:** Methodology, Investigation. **Maria Bošković:** Writing – original draft, Visualization, Methodology. **Zdenko Herceg:** Writing – original draft, Funding acquisition, Conceptualization.

Disclaimer

Where authors are identified as personnel of the International Agency for Research on Cancer/World Health Organization, the authors alone are responsible for the views expressed in this article and they do not necessarily represent the decisions, policy or views of the International Agency for Research on Cancer/World Health Organization.

Funding

This work was supported in part by grants from the Institut National du Cancer (INCa, France), grant numbers INCa-DGOS-Inserm_12563 and INCa-DGOS-INSERM-ITMO cancer_18003) and the Fondation ARC pour la Recherche sur le Cancer (France) and La Ligue Francaise contre le Cancer. The funders of the study had no role in study design, data collection, data analysis, data interpretation or writing of the manuscript.

Declaration of competing interest

The authors declare that they have no known competing financial interests or personal relationships that could have appeared to influence the work reported in this paper.

Appendix A. Supplementary data

Supplementary data to this article can be found online at https://doi.org/10.1016/j.heliyon.2024.e39548.

References

[1] H. Takeshima, T. Ushijima, Accumulation of genetic and epigenetic alterations in normal cells and cancer risk, npj Precis. Oncol. 3 (1) (2019) 7.
[2] Z. Herceg, A. Ghantous, F.F.-L. Chung, Epigenetic epidemiology of cancer, in: K.B. Michels (Ed.), Epigenetic Epidemiology, Springer International Publishing, Cham, 2022, pp. 325–342.
[3] D. Hanahan, Hallmarks of cancer: new dimensions, Cancer Discov. 12 (1) (2022) 31–46.
[4] Z. Herceg, M.P. Lambert, K. van Veldhoven, C. Demetriou, P. Vineis, M.T. Smith, et al., Towards incorporating epigenetic mechanisms into carcinogen identification and evaluation, Carcinogenesis 34 (9) (2013) 1955–1967.
[5] F.F. Chung, Z. Herceg, The promises and challenges of toxico-epigenomics: environmental chemicals and their impacts on the epigenome, Environ. Health Perspect. 128 (1) (2020) 15001.
[6] M.T. Smith, K.Z. Guyton, C.F. Gibbons, J.M. Fritz, C.J. Portier, I. Rusyn, et al., Key characteristics of carcinogens as a basis for organizing data on mechanisms of carcinogenesis, Environ. Health Perspect. 124 (6) (2016) 713–721.
[7] Z. Herceg, A. Ghantous, C.P. Wild, A. Sklias, L. Casati, S.J. Duthie, et al., Roadmap for investigating epigenome deregulation and environmental origins of cancer, Int. J. Cancer 142 (5) (2018) 874–882.
[8] Z. Herceg, T. Vaissiere, Epigenetic mechanisms and cancer: an interface between the environment and the genome, Epigenetics 6 (7) (2011) 804–819.
[9] Z. Yang, A. Jones, M. Widschwendter, A.E. Teschendorff, An integrative pan-cancer-wide analysis of epigenetic enzymes reveals universal patterns of epigenomic deregulation in cancer, Genome Biol. 16 (1) (2015) 140.
[10] A. Halaburkova, V. Cahais, A. Novoloaca, MGdS. Araujo, R. Khoueiry, A. Ghantous, et al., Pan-cancer multi-omics analysis and orthogonal experimental assessment of epigenetic driver genes, Genome Res. 30 (10) (2020) 1517–1532.
[11] A. Youn, K.I. Kim, R. Rabadan, B. Tycko, Y. Shen, S. Wang, A pan-cancer analysis of driver gene mutations, DNA methylation and gene expressions reveals that chromatin remodeling is a major mechanism inducing global changes in cancer epigenomes, BMC Med. Genom. 11 (1) (2018) 98.
[12] Y.-C. Chen, V. Gotea, G. Margolin, L. Elnitski, Significant associations between driver gene mutations and DNA methylation alterations across many cancer types, PLoS Comput. Biol. 13 (11) (2017) e1005840.
[13] S. Turcan, D. Rohle, A. Goenka, L.A. Walsh, F. Fang, E. Yilmaz, et al., IDH1 mutation is sufficient to establish the glioma hypermethylator phenotype, Nature 483 (7390) (2012) 479–483.
[14] R.J. Wright, H.A. Hanson, A tipping point in cancer epidemiology: embracing a life course exposomic framework, Trends in Cancer 8 (4) (2022) 280–282.
[15] M. Carbone, S.T. Arron, B. Beutler, A. Bononi, W. Cavenee, J.E. Cleaver, et al., Tumour predisposition and cancer syndromes as models to study gene–environment interactions, Nat. Rev. Cancer 20 (9) (2020) 533–549.
[16] S.L.W. Tan, S. Chadha, Y. Liu, E. Gabasova, D. Perera, K. Ahmed, et al., A class of environmental and endogenous toxins induces BRCA2 haploinsufficiency and genome instability, Cell 169 (6) (2017) 1105, 18.e15.
[17] IARC Working Group on the Evaluation of Carcinogenic Risks to Humans, Some drinking-water disinfectants and contaminants, including arsenic, IARC Monogr. Eval. Carcinog. Risks Hum. 84 (2004) 1–477.
[18] E.J. Tokar, B.A. Diwan, J.M. Ward, D.A. Delker, M.P. Waalkes, Carcinogenic effects of “whole-life” exposure to inorganic arsenic in CD1 mice, Toxicol. Sci. 119 (1) (2011) 73–83.
[19] B.C. Minatel, A.P. Sage, C. Anderson, R. Hubaux, E.A. Marshall, W.L. Lam, et al., Environmental arsenic exposure: from genetic susceptibility to pathogenesis, Environ. Int. 112 (2018) 183–197.
[20] IARC Working Group on the Evaluation of Carcinogenic Risks to Humans, Arsenic, metals, fibres, and dusts, IARC Monogr. Eval. Carcinog. Risks Hum. 100 (Pt C) (2012) 11–465.
[21] J.F. Reichard, A. Puga, Effects of arsenic exposure on DNA methylation and epigenetic gene regulation, Epigenomics 2 (1) (2010) 87–104.
[22] C.Q. Zhao, M.R. Young, B.A. Diwan, T.P. Coogan, M.P. Waalkes, Association of arsenic-induced malignant transformation with DNA hypomethylation and aberrant gene expression, Proc. Natl. Acad. Sci. U. S. A. 94 (20) (1997) 10907–10912.
[23] L. Benbrahim-Tallaa, R.A. Waterland, M. Styblo, W.E. Achanzar, M.M. Webber, M.P. Waalkes, Molecular events associated with arsenic-induced malignant transformation of human prostatic epithelial cells: aberrant genomic DNA methylation and K-ras oncogene activation, Toxicol. Appl. Pharmacol. 206 (3) (2005) 288–298.
[24] X. Cui, T. Wakai, Y. Shirai, N. Yokoyama, K. Hatakeyama, S. Hirano, Arsenic trioxide inhibits DNA methyltransferase and restores methylation-silenced genes in human liver cancer cells, Hum. Pathol. 37 (3) (2006) 298–311.

[25] J.F. Reichard, M. Schnekenburger, A. Puga, Long term low-dose arsenic exposure induces loss of DNA methylation, Biochem. Biophys. Res. Commun. 352 (1) (2007) 188–192.
[26] K.A. Bailey, R.C. Fry, Arsenic-associated changes to the epigenome: what are the functional consequences? Current Environmental Health Reports 1 (1) (2014) 22–34.
[27] J.R. Pilsner, M.N. Hall, X. Liu, V. Ilievski, V. Slavkovich, D. Levy, et al., Influence of prenatal arsenic exposure and newborn sex on global methylation of cord blood DNA, PLoS One 7 (5) (2012) e37147.
[28] G. Lu, H. Xu, D. Chang, Z. Wu, X. Yao, S. Zhang, et al., Arsenic exposure is associated with DNA hypermethylation of the tumor suppressor gene p16, J. Occup. Med. Toxicol. 9 (1) (2014) 42.
[29] T. Gonzalez-Cortes, R. Recio-Vega, R.C. Lantz, B.T. Chau, DNA methylation of extracellular matrix remodeling genes in children exposed to arsenic, Toxicol. Appl. Pharmacol. 329 (2017) 140–147.
[30] M.J. Aryee, A.E. Jaffe, H. Corrada-Bravo, C. Ladd-Acosta, A.P. Feinberg, K.D. Hansen, et al., Minfi: a flexible and comprehensive Bioconductor package for the analysis of Infinium DNA methylation microarrays, Bioinformatics 30 (10) (2014) 1363–1369.
[31] E.Y. Chen, C.M. Tan, Y. Kou, Q. Duan, Z. Wang, G.V. Meirelles, et al., Enrichr: interactive and collaborative HTML5 gene list enrichment analysis tool, BMC Bioinf. 14 (1) (2013) 128.
[32] Z. Xie, A. Bailey, M.V. Kuleshov, D.J.B. Clarke, J.E. Evangelista, S.L. Jenkins, et al., Gene set knowledge discovery with Enrichr, Current Protocols 1 (3) (2021) e90.
[33] M.V. Kuleshov, M.R. Jones, A.D. Rouillard, N.F. Fernandez, Q. Duan, Z. Wang, et al., Enrichr: a comprehensive gene set enrichment analysis web server 2016 update, Nucleic Acids Res. 44 (W1) (2016) W90–W97.
[34] H. Wickham, ggplot2: Elegant Graphics for Data Analysis, Springer-Verlag New York, 2016.
[35] C. Wilke, *ggridges: Ridgeline Plots in 'ggplot2'*. R package version 0.5.6. https://wilkelab.org/ggridges/.
[36] Y. Zheng, B.T. Joyce, L. Liu, Z. Zhang, W.A. Kibbe, W. Zhang, et al., Prediction of genome-wide DNA methylation in repetitive elements, Nucleic Acids Res. 45 (15) (2017) 8697–8711.
[37] D. Uribe, A. Cardona, D.D. Esposti, M.-P. Cros, C. Cuenin, Z. Herceg, et al., Antiproliferative effects of epigenetic modifier drugs through E-cadherin up-regulation in liver cancer cell lines, Ann. Hepatol. 17 (3) (2018) 444–460.
[38] Z. Awada, L. Bouaoun, R. Nasr, A. Tfayli, C. Cuenin, R. Akika, et al., LINE-1 methylation mediates the inverse association between body mass index and breast cancer risk: a pilot study in the Lebanese population, Environ. Res. 197 (2021) 111094.
[39] A. Sklias, A. Halaburkova, L. Vanzan, N.F. Jimenez, C. Cuenin, L. Bouaoun, et al., Epigenetic remodelling of enhancers in response to estrogen deprivation and re-stimulation, Nucleic Acids Res. 49 (17) (2021) 9738–9754.
[40] V.D. Martinez, W.L. Lam, Health effects associated with pre- and perinatal exposure to arsenic, Front. Genet. 12 (2021) 664717.
[41] B. Zhu, A. Lindsey, N. Li, K. Lee, V. Ramirez-Alcantara, J.C. Canzoneri, et al., Phosphodiesterase 10A is overexpressed in lung tumor cells and inhibitors selectively suppress growth by blocking β-catenin and MAPK signaling, Oncotarget 8 (41) (2017).
[42] S. Catalano, S. Panza, G. Augimeri, C. Giordano, R. Malivindi, L. Gelsomino, et al., Phosphodiesterase 5 (PDE5) is highly expressed in cancer-associated fibroblasts and enhances breast tumor progression, Cancers 11 (11) (2019) 1740.
[43] G.A. Piazza, A. Ward, X. Chen, Y. Maxuitenko, A. Coley, N.S. Aboelella, et al., PDE5 and PDE10 inhibition activates cGMP/PKG signaling to block Wnt/β-catenin transcription, cancer cell growth, and tumor immunity, Drug Discov. Today 25 (8) (2020) 1521–1527.
[44] S. Chen, J. Chen, W. Du, D.M. Mickelsen, H. Shi, H. Yu, et al., PDE10A inactivation prevents doxorubicin-induced cardiotoxicity and tumor growth, Circ. Res. 133 (2) (2023) 138–157.
[45] Y. Cheng, Y. Zhu, J. Xu, M. Yang, P. Chen, W. Xu, et al., PKN2 in colon cancer cells inhibits M2 phenotype polarization of tumor-associated macrophages via regulating DUSP6-Erk1/2 pathway, Mol. Cancer 17 (1) (2018) 13.
[46] Y. Tomita, N. Marchenko, S. Erster, A. Nemajerova, A. Dehner, C. Klein, et al., WT p53, but not tumor-derived mutants, bind to Bcl2 via the DNA binding domain and induce mitochondrial permeabilization, J. Biol. Chem. 281 (13) (2006) 8600–8606.
[47] W. Hill, E.L. Lim, C.E. Weeden, C. Lee, M. Augustine, K. Chen, et al., Lung adenocarcinoma promotion by air pollutants, Nature 616 (7955) (2023) 159–167.
[48] B.J. Aubrey, G.L. Kelly, A. Janic, M.J. Herold, A. Strasser, How does p53 induce apoptosis and how does this relate to p53-mediated tumour suppression? Cell Death Differ. 25 (1) (2018) 104–113.
[49] M. Zhang, G. Zhuang, X. Sun, Y. Shen, W. Wang, Q. Li, et al., TP53 mutation-mediated genomic instability induces the evolution of chemoresistance and recurrence in epithelial ovarian cancer, Diagn. Pathol. 12 (1) (2017) 16.
[50] B.S. Tan, K.H. Tiong, H.L. Choo, F. Fei-Lei Chung, L.W. Hii, S.H. Tan, et al., Mutant p53-R273H mediates cancer cell survival and anoikis resistance through AKT-dependent suppression of BCL2-modifying factor (BMF), Cell Death Dis. 6 (7) (2015) e1826–e.
[51] W. Hanel, U.M. Moll, Links between mutant p53 and genomic instability, J. Cell. Biochem. 113 (2) (2012) 433–439.
[52] F. Ma, Y.Y. Lei, M.G. Ding, L.H. Luo, Y.C. Xie, X.L. Liu, LncRNA NEAT1 interacted with DNMT1 to regulate malignant phenotype of cancer cell and cytotoxic T cell infiltration via epigenetic inhibition of p53, cGAS, and STING in lung cancer, Front. Genet. 11 (2020) 250.
[53] B. Dhaka, R. Sabarinathan, Differential chromatin accessibility landscape of gain-of-function mutant p53 tumours, BMC Cancer 21 (1) (2021) 669.
[54] M.S. Lawrence, P. Stojanov, P. Polak, G.V. Kryukov, K. Cibulskis, A. Sivachenko, et al., Mutational heterogeneity in cancer and the search for new cancer-associated genes, Nature 499 (7457) (2013) 214–218.
[55] B. Schuster-Bockler, B. Lehner, Chromatin organization is a major influence on regional mutation rates in human cancer cells, Nature 488 (7412) (2012) 504–507.
[56] R. Murr, J.I. Loizou, Y.G. Yang, C. Cuenin, H. Li, Z.Q. Wang, et al., Histone acetylation by Trrap-Tip60 modulates loading of repair proteins and repair of DNA double-strand breaks, Nat. Cell Biol. 8 (1) (2006) 91–99.
[57] A. Tovy, A. Spiro, R. McCarthy, Z. Shipony, Y. Aylon, K. Allton, et al., Corrigendum: p53 is essential for DNA methylation homeostasis in naive embryonic stem cells, and its loss promotes clonal heterogeneity, Genes Dev. 32 (19–20) (2018) 1358.
[58] L.Y. Lim, N. Vidnovic, L.W. Ellisen, C.O. Leong, Mutant p53 mediates survival of breast cancer cells, Br. J. Cancer 101 (9) (2009) 1606–1612.
[59] A. Polotskaia, G. Xiao, K. Reynoso, C. Martin, W.G. Qiu, R.C. Hendrickson, et al., Proteome-wide analysis of mutant p53 targets in breast cancer identifies new levels of gain-of-function that influence PARP, PCNA, and MCM4, Proc Natl Acad Sci U S A. 112 (11) (2015) E1220–E1229.